Demonstration of a Novel Atomic Beam Splitter

John Lawall* and Mara Prentiss
Lyman Laboratory of Physics, Harvard University, Cambridge, Massachusetts 02138
(Received 16 April 1993)

We have demonstrated a novel beam splitter for atoms. The $J=1$ to $J=0$ system in metastable helium has two independent "dark" states which are radiatively stable. By preparing atoms in the two "dark" states of the 2^3S_1 level and passing them through a sequence of partially overlapping laser beams tuned to the 2^3S_1-2^3P_0 transition, we cause the atoms in one "dark" state to be deflected by integral multiples of $2\hbar k$, while the atoms in the other "dark" state are undeflected. The excited 2^3P_0 state is not populated, so the process is unaffected by spontaneous emission. We have observed up to 90% coherent momentum transfer with $4\hbar k$ deflection. We conclude by describing how one might construct an atom interferometer based on these "dark state" beam splitters.

PACS numbers: 42.50.Vk, 07.60.Ly, 35.80.+s

Atom interferometers have been demonstrated in a number of different labs [1]. Such interferometers may offer dramatically enhanced sensitivity to measurements of departures from inertial reference frames. For similar geometries, the ratio of the gyroscopic sensitivity [2] of an atom interferometer to a light interferometer is $\approx 10^{10}$. However, the sensitivity is also proportional to the enclosed area, and atom interferometers presently have areas $\approx 10^{-5}$ m^2 because the beam splitters used in these interferometers give very small momentum splittings. In this paper, we present a beam splitter which is capable of deflection through a large angle, deflects atoms into exactly two distinct momentum states, and is robust with respect to experimental parameters.

The beam splitter uses laser induced adiabatic passage to coherently transfer atoms to higher momentum states. The use of temporally overlapping laser pulses to induce adiabatic passage has been demonstrated previously [3]. Its capacity for momentum transfer was first noted by Marte, Zoller, and Hall [4], who described an atomic mirror based on the 2^3S_1-2^3P_1 transition in metastable helium. In this paper, we demonstrate [5] a state-selective atomic beam splitter using the 2^3S_1-2^3P_0 transition.

The relevant atomic levels and a schematic of our experimental setup are shown in Fig. 1. An atomic beam propagating along $\hat{\mathbf{x}}$ crosses a pair of counterpropagating, circularly polarized laser beams. The laser beams are spatially displaced along the atomic beam so that the atom sees the field in a sequence of two overlapping pulses. The direction of propagation of the first laser beam defines our quantization axis $\hat{\mathbf{z}}$. The states are coupled by the laser beams, whose electric fields

$$\begin{aligned} \mathbf{E}_1 &= \mathrm{Re}E_-(x)e^{i(kz-\omega t)}\hat{\epsilon}_-\,, \\ \mathbf{E}_2 &= \mathrm{Re}E_+(x)e^{i(-kz-\omega t)}\hat{\epsilon}_+\,, \\ E_\pm(x) &= E_0 e^{-(x\mp x_0)^2/\omega_0^2} \end{aligned} \tag{1}$$

are treated classically. The ellipticity of the light may be described by $\theta=\tan^{-1}(E_+/E_-)$, and smoothly rotates from 0 to $\pi/2$ as the atom crosses the laser interaction region.

Here we treat the external as well as internal atomic coordinates quantum mechanically. In the absence of spontaneous emission, the set of states

$$\{|g,-1,p-\hbar k\rangle,|g,0,p'\rangle,|g,+1,p+\hbar k\rangle,|e,0,p\rangle\}$$

is closed, where the quantum numbers refer to the electronic level, magnetic sublevel, and center-of-mass momentum along $\hat{\mathbf{z}}$, respectively. The internal and external degrees of freedom are related by absorption and stimulated emission processes. Diagonalization of the interaction-picture Hamiltonian in this basis yields two degenerate, orthogonal eigenfunctions with no component of the excited state that is thus immune from spontaneous decay ("dark" states). For zero detuning from atomic resonance, they may be written as

$$|\phi_0\rangle = |g,0,p'\rangle\,, \tag{2}$$

$$|\phi_\theta\rangle = \cos(\theta)e^{-i\Delta t}|g,-1,p-\hbar k\rangle + \sin(\theta)e^{i\Delta t}|g,+1,p+\hbar k\rangle\,, \tag{3}$$

where $\Delta=kp/m$ is the Doppler shift arising from atomic motion along $\hat{\mathbf{z}}$. $|\phi_0\rangle$ is trivially decoupled from the fields by selection rules. In the cases that the light is pure σ_-

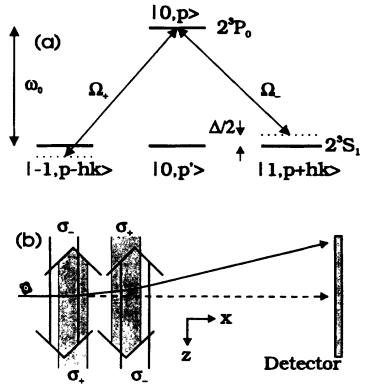

FIG. 1. (a) States of interest coupled by absorption/emission. (b) Experimental schematic.

0031-9007/94/72(7)/993(4)$06.00

or σ_+, $|\phi_\theta\rangle$ simplifies to the state $e^{i\Delta t}|g,-1,p-\hbar k\rangle$ or $e^{-i\Delta t}|g,+1,p+\hbar k\rangle$, respectively. These states, too, are decoupled from the field by selection rules.

The eigenfunctions $|\phi_\theta\rangle$ and $|\phi_0\rangle$ behave differently under transformations of the parameter θ. As the ellipticity of the light rotates slowly from $\theta=0$ to $\pi/2$, an atom initially in the state $|g,-1,p-\hbar k\rangle$ will adiabatically stay in the state $|\phi_\theta\rangle$ and emerge in the state $|g,+1,p+\hbar k\rangle$, where its center-of-mass momentum differs by $2\hbar k$. By contrast, the state $|\phi_0\rangle$ is invariant under transformations of θ, and so an atom prepared in $|\phi_0\rangle$ emerges in the same state, undeflected. Thus, an atom initially prepared in a superposition state $|\psi_i\rangle=a|g,-1,0\rangle+b|g,0,0\rangle$ will emerge in the state $|\psi_f\rangle=ae^{-2i\hbar k^2t/m}e^{i\gamma}|g,+1,2\hbar k\rangle+b|g,0,0\rangle$, its wave function coherently split in momentum space. Here the phase term in front of the deflected component of the (Schrödinger picture) wave function reflects the recoil kinetic energy and a constant term arising from the adiabatic passage. In principle, the process can be repeated indefinitely, and after n cycles the final state will be

$$|\psi_f\rangle=ae^{-2i\hbar n^2k^2t/m}e^{i\gamma'}|g,-(-1)^n,2n\hbar k\rangle+b|g,0,0\rangle.$$

The conditions under which the state $|\psi_\theta\rangle$ rotates adiabatically have been studied by several authors [3,4,6]. A sufficient condition for adiabatic following is [4]

$$\Omega\gg\Gamma,\quad \Omega\gg 1/\tau',\quad \Omega\gg\Delta, \tag{4}$$

where $\Omega=|E_0\hat{\epsilon}\cdot\mathbf{d}|/\hbar$ is the maximum Rabi frequency and τ' is a characteristic time for the passage. We work in He^*, for which the 2^3S_1-2^3P_0 transition saturates at 0.5 mW/cm^2 and has a linewidth $\Gamma=10^7$ s^{-1}, so these parameters are very easy to satisfy experimentally. With a typical beam waist of 2.5 mm, we can achieve a Rabi frequency Ω up to 40Γ. In addition to analytic work, we have done numerical simulations by integrating the Liouville equation describing the evolution of the density matrix for the four-level system with a damping term for spontaneous decay. We assume the Rabi frequencies of the beams are Gaussian pulses with half-width τ and separation 2ϵ. Figure 2 shows representative curves, where the pulse overlap is as shown in Fig. 2(a) ($\epsilon=0.6\tau$). Figures 2(b) and 2(c) assume that the atom was initially prepared in a symmetric coherent superposition of $m_J=-1$ and $m_J=0$, driven by laser fields with $\Omega=10\Gamma$. The population transfer from $m_J=-1$ to $m_J=+1$ is complete, as is the transfer of the coherence between $m_J=-1$ and $m_J=0$ to $m_J=0$ and $m_J=+1$. Figure 2(d) compares the populations in state $m_J=0$ for the situation described above and a case where the laser power has been reduced such that $\Omega=\Gamma$. Here condition (4) is violated. There is significant population of the excited state, and 16% of the population initially in $m_J=-1$ spontaneously decays to the state $m_J=0$. Thus 48% of the population initially in $m_J=-1$ is incoherently scattered.

The experimental apparatus consists of a highly collimated atomic beam, a laser interaction region, and a high resolution detector. Metastable helium is created in a strong, pulsed rf discharge and effuses out of a 5 μm×0.5 mm slit. Measurements of deflection from radiation pressure indicate 93% of the metastable atoms are in the 2^3S_1 state; the remaining 7% in the 2^1S_0 state constitute a small background on the undeflected atoms with $m_J=0$. Collimation is provided by a 15 μm slit 19 cm downstream, resulting in a full-angular spread of 10^{-4} rad ($2\hbar k$). Immediately after the collimating slit is the laser interaction region. A double Mumetal shield and two pairs of Helmholtz coils null the magnetic field within this region to 2.5 mG along the laser beams and less than 0.5 mG perpendicular to them. At the end of a 168 cm free flight region is a Galileo Model 3018 position-sensitive detector. The detector is comprised of a Chevron channel-plate assembly with 8 μm pores separated by 10 μm center-to-center, a phosphor screen, and a fiberoptic light coupler. The green blips of light resulting (P20 phosphor, $\tau=200$ μs), visible to the naked eye, are picked up by a Cohu Model 4110 digital charge-coupled-device (CCD) camera and the resulting images processed with an Epix 4Meg video board. The rf pulses driving the helium discharge are synchronized to the video signal and a 500 μs electronic shutter is used on the camera in order to provide time-of-flight velocity selection, giving $v/\delta v\approx 3$. Images of 12800 pixels are analyzed to find the centroids of the blips of light and record them continuously at 30 Hz. The data acquisition rate is about 6 atoms/s, and complete data runs have over 3600 points. After acquiring a complete image, a histogram is compiled to integrate over the vertical dimension.

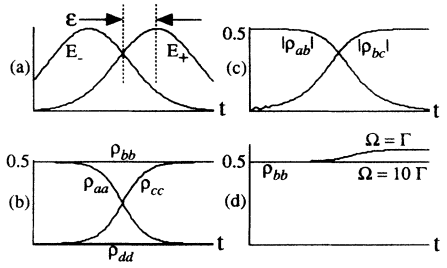

FIG. 2. (a) Electric fields vs time. The half-width of the pulses is defined to be τ. (b)–(d) Density matrix elements vs time where a,b,c refer to the $m_J=-1,0,+1$ ground state sublevels, respectively, and d refers to the excited state.

The LNA laser used to drive the 2^3S_1-2^3P_0 transition represents some improvement over our earlier work [7]. With a nominal 3 W pump on the 514 nm line of an argon-ion pump laser, the power output is 175 mW single mode at 1.083 μm. The laser is locked to an external super-Invar cavity which is in turn locked to a helium discharge cell. The laser beam used for the experiment is on resonance and has a linewidth of about 240 kHz. The laser output is passed through an acousto-optic modulator (AOM) to prevent optical feedback, cleaned up with a spatial filter, expanded, and collimated. The beam profile

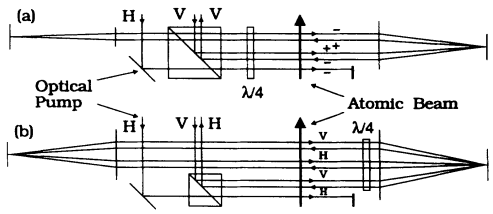

FIG. 3. (a) Optical setup for $4\hbar k$ deflection using circular polarization. The $\pm$ indicates the helicity. (b) Setup for $6\hbar k$ deflection using linear polarization.

is Gaussian as measured with a CCD camera and has a waist ω_0 of 2.5 mm. Our scheme for acquiring $4\hbar k$ of transverse momentum is shown in Fig. 3(a). The polarizing beam splitter and zero-order quarter wave plate are used to define the polarizations. A double catseye setup allows the beams to propagate parallel with easily controlled overlap. The lenses and vacuum chamber windows are antireflection (AR) coated, and the catseyes are not significantly birefringent. Indeed, any deterioration in polarization due to the first catseye and vacuum windows is "cleaned up" by the polarizing cube, as is the effect of any birefringence arising from the second catseye.

In our apparatus, we do not start with a coherent superposition of the $m_J=-1$ and $m_J=0$ sublevels. Instead, we optically pump the atoms into an incoherent mixture of $m_J=0$ and $m_J=-1$ by means of σ_- light. The two atomic beams emerging from our laser region are thus not coherent. Nevertheless, we are able to study the coherence of the adiabatic momentum transfer by observation of the final atomic momentum distribution. For example, if the overlap between the σ_+ and σ_- beams is too small, we anticipate an incoherent process in which the (first) σ_- beam has no effect on the atoms, and the subsequent σ_+ beam optically pumps those atoms initially in $m_J=-1$ equally into the $m_J=0$ and $m_J=+1$ sublevels. Each such process results in an average $\frac{1}{2}\hbar k$ momentum transfer with considerable variance as it is governed by spontaneous emission. Thus the momentum acquired will be smaller than for the coherent process and its distribution more diffuse. Furthermore, if the process is repeated, the atoms will become pumped into the $m_J=0$ sublevel and the momentum transfer will become even smaller. By comparing the observed momentum transfer to simulations, we can deduce the fraction of atoms which are coherently deflected.

Figure 4(a) shows experimental results for the parameters $\Omega=3.9\Gamma$ and $\epsilon/\tau=0.6$. The spikes in the data are an artifact of the detection whose root is believed to be in the CCD camera. The theoretical curve assumes that 90% of the atoms are deflected coherently and 10% scattered incoherently. The fraction of coherent deflection is the only adjustable parameter in the theoretical curve.

The dependence of the momentum transfer on beam overlap is shown in Fig. 5(c). For relatively large beam overlaps (corresponding to values $\epsilon<0.4\tau$ as defined in

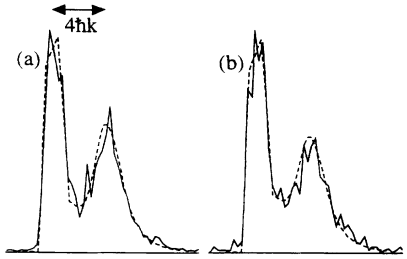

FIG. 4. (a) $4\hbar k$ deflection using circular polarization. (b) $4\hbar k$ deflection using linear polarization. The width of the deflected peaks is due to the longitudinal atomic velocity distribution. The dashed lines are theory.

Fig. 2), the distance over which the polarization of the laser light rotates from σ_- to σ_+ exceeds the beam waists and the process fails due to the imperfections in the beam quality and the proximity of the successive laser interaction zones. As the overlap is reduced the fraction of atoms coherently deflected is increased until eventually the laser power is too small in the region of overlap and it diminishes again. The fraction of coherent transfer that we infer from the data is in reasonably good agreement with analytic work that we have done.

The dependence of the momentum transfer process on the laser power is next shown in Fig. 5(d). Here we expect that the process should be incoherent for laser powers such that $\Omega\leq\Gamma$, and become better and better as the Rabi frequency is raised. These expectations are indeed fulfilled for $\Omega<4\Gamma$, but as the laser power is increased much past this point the coherence is destroyed. We believe that this is a consequence of stray reflections off AR coated surfaces. If so, avoiding normal incidence on the vacuum windows to reduce the amount of scattered light should allow deflections of more than $8\hbar k$ with close to 100% coherent momentum transfer.

We also measured the angular dependence of our result by incrementally sweeping the angle of the entire optical arrangement. This has the effect of introducing an additional differential Doppler shift Δ (Fig. 1) which [Eq. (4)] must be compensated by raising the laser power. In our case the Doppler shift is about 1.05Γ/mrad. The angle at which the laser was perpendicular to the atomic beam was first determined by using 1D optical molasses on the 2^3S_1-2^3P_2 transition. At a Rabi frequency of

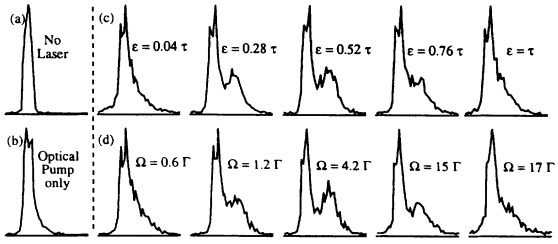

FIG. 5. (a) Undeflected beam (b) deflection by optical pump. (c) Scan of beam overlap for fixed laser power $\Omega=1.7\Gamma$. (d) Scan of power for fixed beam overlap $\epsilon=0.6\tau$.

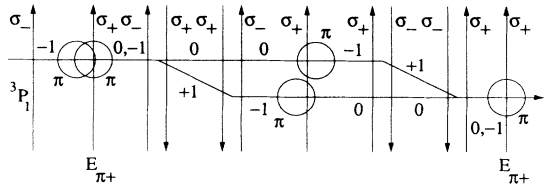

FIG. 6. Possible realization of a dark-state interferometer for He*. The laser beam at the far left is tuned to the 2^3S_1-2^3P_1 transition; all others are tuned to the 2^3S_1-2^3P_0 transition. The circles represent π-polarized Gaussian laser beams propagating perpendicular to the page. The figures $\{0, \pm 1\}$ indicate the magnetic sublevel.

$\Omega = 3.9\Gamma$, we observed 90% coherent momentum transfer at normal incidence, and over 70% coherence over an angular range of 0.38 mrad. We found as expected that the loss of coherent transfer at the larger angles could be compensated by raising the laser power. At an angle of 0.27 mrad, we were able to increase the coherent momentum transfer from 40% to 70% by raising the laser power from 3.9Γ to 6.2Γ, and at 0.4 mrad we increased it from 20% to 60% by raising the laser power from 3.9Γ to 9.1Γ. Again, these results agree well with our analytic predictions.

Finally, we varied the experimental arrangement to an orthogonal linear rather than circular basis. Here the "dark states" in which the atoms enter and exit the regions of adiabatic passage are the symmetric and antisymmetric linear combinations of the $m_J = -1$ and $m_J = +1$ sublevels, rather than eigenstates of J_z, and the ellipticity parameter θ is swept from $-\pi/4$ to $\pi/4$ instead of from 0 to $\pi/2$. The process is still accompanied by an absorption/stimulated emission cycle, and experimental results are shown in Fig. 4(b), where they fit well to a theoretical curve assuming an 80% coherent momentum transfer. A schematic of the optics for a triple pass to give $6\hbar k$ deflection using linearly polarized light is shown in Fig. 3(b). We observe a $6\hbar k$ process using exactly this scheme, although the experimental conditions were less favorable and only about 60% of the momentum transfer is coherent. We note that for linear polarization the retroreflected laser beam is polarized orthogonally to the outgoing one, so no AOM is required.

These ideas can be extended to flip the atomic state from $m_J = \pm 1$ to $m_J = 0$ and vice versa by the use of π-polarized light. This would be of interest in making an interferometer in a parallelogram arrangement so that the accumulated phase shifts from the recoil mentioned earlier would cancel. In order to rotate the population out of the $m_J = 0$ sublevel into the $m_J = 1$ sublevel, for example, one would use an initial σ_- beam, followed by a partially overlapping π-polarized beam propagating in the y direction. The atom would absorb a photon from the π-polarized beam and reemit into the σ_- beam, and the population would be adiabatically transferred from $m_J = 0$ to $m_J = 1$. Finally, we note that with the addition of a second LNA laser tuned to the 2^3S_1-2^3P_1 transition, one has all the elements necessary to realize a beam of atoms in a *coherent* superposition of the $m_J = 0$ and $m_J = -1$ states which could be used in a "dark-state" atom interferometer. One possible realization of such an interferometer in the parallelogram configuration is shown in Fig. 6. First, the atomic beam would be optically pumped into the $m_J = -1$ state by means of σ_- light on the 2^3S_1-2^3P_1 transition, which has only a *single* dark state. At this point, the atomic beam would pass through a region of partially overlapping laser beams tuned to the 2^3S_1-2^3P_0 transition in which the first beam would be π polarized and the second "beam" would be comprised of σ_+ and π-polarized beams of equal intensities:

$$\mathbf{E}_{\pi+} = \mathrm{Re}[E_\pi(x)e^{i(ky-\omega t)}\hat{\mathbf{z}} + E_+(x)e^{i(kz-\omega t)}\hat{\boldsymbol{\epsilon}}_+]. \quad (5)$$

Thus, the atom would be adiabatically rotated into a symmetric linear combination of the states $m_J = -1$ and $m_J = 0$. This state has the property that it is a dark state for the field $\mathbf{E}_{\pi+}$, which means that $\mathbf{E}_{\pi+}$ could be used to probe the atom after it emerged from the interferometer. The beam splitters in the interferometer would maintain the atoms in dark states for π and $\sigma_\pm$ light separately, but a differential phase shift occurring within the interferometer would rotate the atom out of the dark state for $\mathbf{E}_{\pi+}$ and the resulting absorption would provide an easily detected signal. An alternative, simpler approach to generating and detecting the coherence would be to optically pump directly with a superposition of σ_- and π-polarized beams tuned to the 2^3S_1-2^3P_1 transition. This same superposition beam would be used for the detection as well. Many variations are possible; the future of dark state interferometry looks quite bright.

We are deeply grateful to Frank Pipkin for support and guidance during the preliminary stages of this work. We would like to thank Ed Hagley and Karl Berggren for experimental help, and one of our referees for suggesting the alternative method of generating the coherence described in the previous paragraph. This work is supported by NSF Grant No. PHY-9016886 and ONR Grant No. ONR-N0014-91-J-1808.

*Present address: Laboratoire de Spectroscopie Hertzienne de l'ENS, 24 rue Lhomond, 75005 Paris, France.

[1] F. Riehle, T. Kisters, A. Witte, J. Helmcke, and C. Borde, Phys. Rev. Lett. **67**, 177 (1991); D. Keith, C. Ekstrom, Q. Turchette, and D. Pritchard, Phys. Rev. Lett. **66**, 2693 (1991); O. Carnal and J. Mlynek, Phys. Rev. Lett. **66**, 2689 (1991).

[2] J. F. Clauser, Physica (Amsterdam) **151B**, 262 (1988).

[3] U. Gaubatz, P. Rudecki, S. Schiemann, and K. Bergmann, J. Chem. Phys. **92**, 5363 (1990).

[4] P. Marte, P. Zoller, and J. L. Hall, Phys. Rev. A **44**, R4118 (1991).

[5] See also L. S. Goldner *et al.*, following Letter, Phys. Rev. Lett. **72**, 997 (1994).

[6] J. R. Kuklinski, U. Gaubatz, F. T. Hioe, and K. Bergmann, Phys. Rev. A **40**, 6741 (1989); G. W. Coulston and K. Bergmann, J. Chem. Phys. **96**, 3467 (1992).

[7] P. Zhao, J. R. Lawall, and F. M. Pipkin, Phys. Rev. Lett. **66**, 592 (1991).

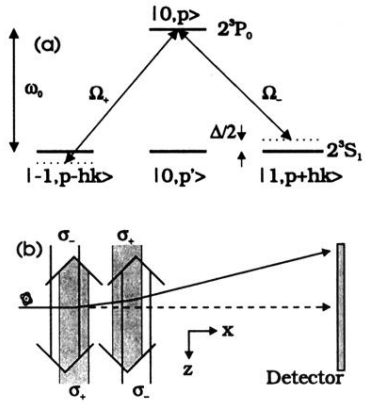

FIG. 1. (a) States of interest coupled by absorption/emission. (b) Experimental schematic.